

Non-adiabatic Non-Hermitian Sensing enabled by Criticality-Enhanced Topological Tunneling

Teng Liu,¹ Xiaohang Zhang,¹ Jiawei Zhang,^{1,2,3,*} and Le Luo^{1,2,3,4,5,†}

¹*School of Physics and Astronomy, Sun Yat-sen University, Zhuhai 519082, China*

²*Guangdong Provincial Key Laboratory of Quantum Metrology and Sensing, Sun Yat-sen University, Zhuhai 519082, China*

³*Shenzhen Research Institute of Sun Yat-Sen University, Shenzhen 518057, China*

⁴*Quantum Science Center of Guangdong-Hong Kong-Macao Greater Bay Area, Shenzhen 518048, China*

⁵*State Key Laboratory of Optoelectronic Materials and Technologies, Sun Yat-sen University, Guangzhou 510275, China*

Non-Hermitian sensing is an intriguing mechanism that utilizes the nonlinear responses near the exceptional points (EPs) to amplify external perturbations with unprecedented precision. While promising transformative sensitivity, existing approaches face stringent limitations due to their reliance on quasi-static state responses and simultaneously encountering divergent noise arising from eigenstate collapse. Here, we propose a non-adiabatic sensing paradigm leveraging parameter-sensitive non-Hermitian tunneling, which surmounts the limitations of adiabatic approaches. This sensitivity, under a metric transformation, is governed by the phase change rate—modulated by the external signal—with geometric amplification, manifesting (i) criticality enhancement (quantum metric divergence near EPs) and (ii) chiral selectivity governed by path- and state-dependent imaginary intraband Berry connections. Experimentally, we validate this paradigm through direct measurements of the Fisher information on a trapped-ion platform. This work establishes a pathway to practical non-Hermitian sensing with non-Abelian non-adiabatic processes.

Non-Hermitian systems, particularly those exhibiting parity-time (\mathcal{PT}) symmetry, host exceptional points (EPs) at which energy eigenvalues and their corresponding eigenstates coalesce [1–3]. Extensive studies demonstrate that, in contrast to Hermitian systems, the eigenfrequency splitting ($\Delta\omega$) near EPs adheres to a nonlinear scaling relation $\Delta\omega \sim \epsilon^{1/N}$, where N denotes the EP order [4, 5]. This scaling confers significant sensitivity enhancement for weak-signal detection, thereby establishing EPs as the predominant framework for non-Hermitian sensing. The characteristic sensitivity scaling has been experimentally validated across diverse platforms, including classical optical and acoustic systems [6–9], electronic circuit systems [10–12], and quantum systems [13–15]. Nevertheless, conventional EP-based sensing critically depends on the static spectral structure proximate to EPs. This approach faces significant challenges stemming from an inherent conflict: The pursuit of high sensitivity to weak signals is compromised by concurrent noise amplification and systemic instability near EPs [16, 17]. Thus, emerging paradigms for next-generation non-Hermitian sensing prioritize strategies that either bypass EP reliance [18] or circumvent adiabatic constraints in transient dynamic response regimes.

Recent studies have shown that during the encirclement of EPs, non-Hermitian systems undergo non-adiabatic transitions between eigenstates, resulting in chiral and non-reciprocal topological state transfer [19–24]. While such tunneling is often attributed to imaginary energy eigenvalues arising from non-Hermiticity, this interpretation alone remains incomplete. Two distinct mechanisms cooperate during dynamical EP encircling: one driven by imaginary energy spectra that causes exponential population transfer between states, and another of topological origin, arising from eigenstate coalescence at the EP, which induces non-adiabatic state switching even in the absence of imaginary eigenvalues [25, 26]. The latter mechanism is particularly crucial in \mathcal{PT} -symmetric systems below the phase transition point, where no imagi-

nary eigenvalues exist, yet robust tunneling is still observed. This confirms that eigenstate topology—not solely imaginary energy—governs the non-adiabatic dynamics near EPs. However, the sensitivity of this tunneling process to specific parameter choices, especially under preserved \mathcal{PT} -symmetry, remains an open question essential for applications requiring quantum-state controllability.

In this work, we address this question by establishing a quantum-geometric framework that reveals how the parameter sensitivity of tunneling near EPs is fundamentally governed by the Berry connection through quantum metric transformations. We demonstrate analytically that this sensitivity depends explicitly on the phase change rate—an externally controllable quantity—and is enhanced by the critical divergence of the quantum metric tensor dictated by the interband Berry connection. Furthermore, the sensitivity exhibits topological chirality and non-reciprocity, arising from the sign-selective response of the intraband Berry connection to the phase change rate. In contrast to the dynamical tunneling governed by a finite gap in the Landau-Zener model [27–30], the tunneling near exceptional points is geometrically enabled by the critical divergence of the quantum metric. For the first time, we explore the framework of non-Hermitian sensing via the Berry connection in the non-adiabatic regime, and then experimentally demonstrate how the quantum geometry of non-Hermitian systems can be harnessed to improve the sensitivity. This work establishes a new paradigm that leverages the intrinsic geometric properties of non-Hermitian systems, opening pathways toward topological quantum sensing.

Metric transformation of a \mathcal{PT} -symmetric system.— The system's response to the signal is considered within a parameter-modulated \mathcal{PT} -symmetric non-Hermitian Hamiltonian $H_{\mathcal{PT}}(t) = i\gamma\sigma_z + J(t)\cos[\Phi(t)]\sigma_x + J(t)\sin[\Phi(t)]\sigma_y$ where $\Phi(t)$ is the time-dependent phase, $J(t)$ is the modulated Rabi strength, γ is the strength of gain (loss), and $\sigma_{x,y,z}$ are the Pauli matrices. The corresponding energy level model is

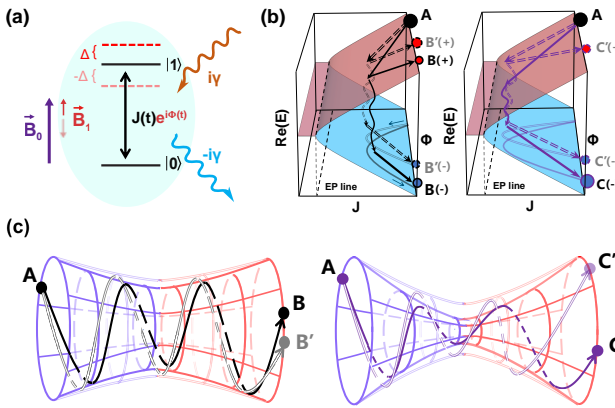


FIG. 1. Non-Hermitian tunneling sensing schematic diagram. (a) Schematic diagram of the energy levels of the non-Hermitian Hamiltonian $H_{\mathcal{PT}}(t)$. The shift of energy levels Δ induced by the external field under measurement is reflected in the variation of the coupling phase $\Phi(t)$ within the Hamiltonian. Here, $J(t)$ is the time-dependent Rabi strength. (b) Schematic diagram of non-Hermitian tunneling. The left (right) panel illustrates tunneling under J and Φ modulation in $H_{\mathcal{PT}}$ far from (near) the EP line. The modulated J is first set near, then far from the EP line. Here, the red (blue) surface represents eigenstates with positive (negative) eigenenergies E ; the dashed (solid) arrow indicates slow (fast) Φ variation ($\dot{\Phi}(t)$); the bottom curve shows the projection of tunneling trajectories; Here, circle A denotes the initial state; B (C) and B' (C') denote the output states. The “+” and “-” represent the two eigenstate branches in the final state, respectively, and the size of each circle denotes the occupation of each branch. (c) Schematic diagram of non-Hermitian tunneling induced by the quantum metric where the left (right) panel depicts tunneling dynamics far from (near) the EPs, corresponding to the small (large) quantum metric. The circular cross-section represents the state space. The blue and red surfaces represent the geometric gain and loss areas, respectively. The corresponding solid and hollow trajectory lines indicate slight variations in $\dot{\Phi}(t)$. This quantum metric provides amplification coupled with $\dot{\Phi}(t)$.

shown in Fig. 1(a). Under the rotating frame transformation, the variation of parameter

$$\Phi(t) = \int_0^t \Delta(\tau) d\tau \quad (1)$$

manifests as the level shift Δ influenced by external fields. Under the $J(t) > \gamma$ condition, this Hamiltonian $H_{\mathcal{PT}}(t)$ allows that the level-shifted system can still be represented in a \mathcal{PT} -symmetric manner.

In such a non-Hermitian evolution, parameter-sensitive tunneling occurs, where faster Φ variation and closer proximity to the EP enhance tunneling probability, as shown in Fig. 1(b). To analytically analyze the sensitivity, we examine this transient response through the quantum metric framework, owing to the occurrence of eigenstates closure near EPs. However, defining quantum geometry in non-Hermitian systems presents challenges, as their eigenstates are generally non-orthogonal. The conventional approach is to introduce a biorthogonal basis. Here, attributed to the maintained symme-

try of $H_{\mathcal{PT}}(t)$, we adopt instead the metric of the \mathcal{CPT} inner product to render the eigenstates of the Hamiltonian complete and orthogonal. Here, $\mathcal{P} = \sigma_x$ and \mathcal{T} is complex conjugation. Unlike previous works [31–33], we introduce a time-dependent metric $\mathcal{C}(t)$,

$$\mathcal{C}(t) = \begin{pmatrix} \frac{i\gamma \exp(-i\Phi(t))}{\sqrt{J(t)^2 - \gamma^2}} & \frac{J(t)}{\sqrt{J(t)^2 - \gamma^2}} \\ \frac{J(t)}{\sqrt{J(t)^2 - \gamma^2}} & \frac{i\gamma \exp(i\Phi(t))}{\sqrt{J(t)^2 - \gamma^2}} \end{pmatrix}, \quad (2)$$

which ensures that the eigenstates $|\phi_{1,2}(t)\rangle$ remain orthogonal and normalized at each moment, i.e., $\langle\phi_{1,2}(t)|\phi_{2,1}(t)\rangle^{\mathcal{CPT}} = 0$, and $\langle\phi_{1,2}(t)|\phi_{1,2}(t)\rangle^{\mathcal{CPT}} = 1$. The instantaneous \mathcal{CPT} inner product is defined as $\langle a | b \rangle^{\mathcal{CPT}} = \langle a | \mathcal{P}^T \mathcal{C}(t)^T | b \rangle$. Thus, we can choose $\{|\phi_{1,2}\rangle\}$ as a complete set of basis vectors. The evolved state is expressed as $|\psi(t)\rangle = \alpha_1(t)|\phi_1(t)\rangle + \alpha_2(t)|\phi_2(t)\rangle$. Using the new metric, the state evolution under parameter modulation can be written as

$$\frac{d}{dt} \alpha_m(t) = i \sum_{n=1}^n [\mathcal{A}_{mn}^{\mathcal{CPT}}(t) - \mathcal{H}_{mn}^{\mathcal{CPT}}(t)] \alpha_n(t), \quad (3)$$

where $m, n \in \{1, 2\}$, $\mathcal{H}_{mn}^{\mathcal{CPT}} = \langle\phi_m(t)|H_{\mathcal{PT}}(t)|\phi_n(t)\rangle^{\mathcal{CPT}}$ are the elements of the dynamical part matrix $\mathcal{H}^{\mathcal{CPT}}$, and $\mathcal{A}_{mn}^{\mathcal{CPT}}(t) = i \langle\phi_m(t)|(\partial/dt)|\phi_n(t)\rangle^{\mathcal{CPT}}$, known as the non-Abelian Berry connection, are the elements of the geometric part $\mathcal{A}^{\mathcal{CPT}}$ (see Supplemental Material (SM) [34] for details). It is noteworthy that, under metric transformation, Eq.(3) describes a geometric process in a non-Hermitian Hilbert space with a twisted mapping relationship to the Hermitian space [33]. Different from previous studies based on the dynamical process induced by the imaginary part of eigenenergies near EPs, we demonstrate that the sensitivity of this tunneling (the \mathcal{PT} -symmetry is maintained and eigenenergies keep real) is governed by the critical quantum metric tensor within the non-Hermitian quantum geometric tensor (NH-QGT).

NH-QGT and critical effects.— The gauge-invariant quantum geometric tensor $\mathcal{T}_{ij}^{\mathcal{CPT}}$ for $H_{\mathcal{PT}}(t)$ can be defined as $\mathcal{T}_{ij}^{n\mathcal{CPT}} = \langle\partial_i\phi_n|\partial_j\phi_n\rangle^{\mathcal{CPT}} - \mathcal{A}_i^{n\mathcal{CPT}}\mathcal{A}_j^{n\mathcal{CPT}}$, where $\mathcal{A}_j^{n\mathcal{CPT}} = \langle\phi_n|i\partial_j|\phi_n\rangle^{\mathcal{CPT}}$ is known as the intraband Berry connection, the index n represents the order of eigenstates, and indices i and j represent the order of time-evolving parameters. The real part of the QGT, known as the quantum metric tensor, is given by $g_{ij}^{\mathcal{CPT}} \equiv \text{Re } \mathcal{T}_{ij}^{\mathcal{CPT}} = \text{Re} \sum_{m \neq n} \mathcal{A}_i^{nm\mathcal{CPT}} \mathcal{A}_j^{mn\mathcal{CPT}}$, where $\mathcal{A}_j^{mn\mathcal{CPT}} = \langle\phi_m|i\partial_j|\phi_n\rangle^{\mathcal{CPT}}$ is the interband Berry connection (see SM [34] for more details). The $g_{ij}^{\mathcal{CPT}}$ defines the *distance* between infinitesimally close quantum states in parameter space and quantifies their distinguishability under small parameter variations. Specifically, a larger local $g_{ij}^{\mathcal{CPT}}$ makes adiabaticity harder to maintain due to enhanced sensitivity to parameter variations [26, 35], as illustrated in Fig. 1(c). In our sensing model $H_{\mathcal{PT}}(t)$, $g_{ij}^{\mathcal{CPT}}$ can be expressed

$$g_{ij}^{\mathcal{CPT}}(t) = \frac{1}{2\sqrt{1 - \beta^2(t)}} \zeta(t) - \frac{1}{2(1 - \beta^2(t))^{3/2}} \zeta(t)^{-1}, \quad (4)$$

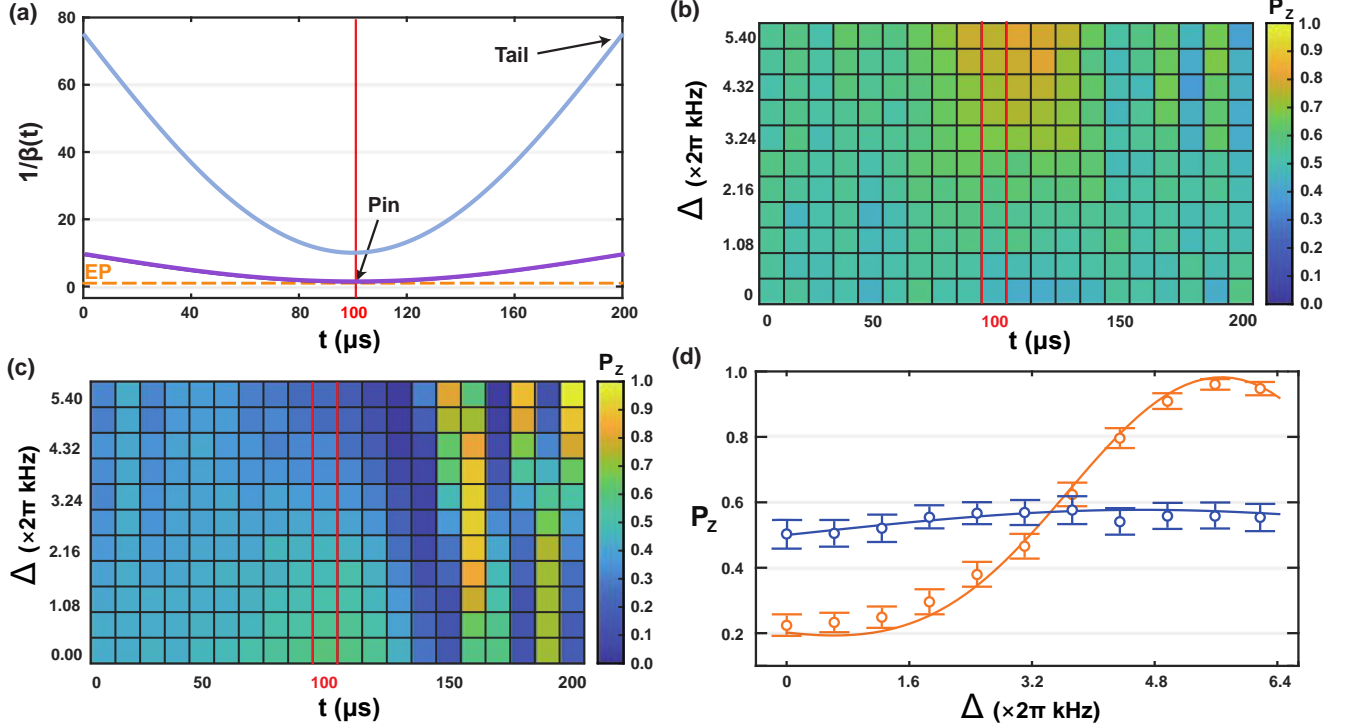


FIG. 2. Experimental results of non-Hermitian tunneling. (a) Experimental parameter modulation scheme. The horizontal orange dashed line indicates the EP line ($\beta = 1$). The vertical red line marks $\tau_p = 100 \mu\text{s}$, where the “pin” is closest to the EP line. The upper blue solid line represents $\beta_p = 0.1$, while the lower purple solid line corresponds to $\beta_p = 0.8$. (b) Evolution of P_z and its response characteristics under different $\dot{\Phi}$ conditions in the Hermitian case (e.g., $\beta_p=0$). The red box marks the position of the pin ($\tau_p = 100 \mu\text{s}$). (c) Evolution of P_z and its response characteristics under different $\dot{\Phi}$ conditions in the non-Hermitian case ($\beta_p=0.75$). (d) Experimental measurements of the final-state P_z population under different parameter sweep rates $d\Phi/dt$. The orange points represent the non-Hermitian case ($\beta_p = 0.75$), while the blue points correspond to the Hermitian case ($\beta_p = 0$). The non-Hermitian regime shows higher parameter sensitivity, confirming enhanced CFI.

where $\beta(t) = \gamma/J(t)$ is the relative dissipation rate, and $\zeta(t) = \dot{\Phi}(t)/\dot{\beta}(t)$ is the EPs-independent parameter, which can be modulated by the controlled parameter $\dot{\beta}(t) = d\beta(t)/dt$. For a scanning-type modulation protocol with $\beta(t)$ (e.g., first approaching then departing from the EPs), the maximum value $\beta^{\max}(t = \tau_p)$ occurs at the position closest to the EPs, where $\dot{\beta}(\tau_p) = 0$. In this case, the first term of $g_{ij}^{\mathcal{CPT}}(t)$ dominates [34]. Thus, we can obtain an EPs-dependent amplification factor $\xi(t) = 1/(2\sqrt{1 - \beta^2(t)})$, i.e., $g_{ij}^{\mathcal{CPT}}(t) \approx \xi(t)\zeta(t)$. In the \mathcal{PT} -symmetric regime, when $\beta^{\max}(\tau_p) \rightarrow 1$, driving $\xi(\tau_p) \rightarrow \infty$, the metric tensor $g_{ij}^{\mathcal{CPT}}$ diverges, exhibiting criticality-enhanced sensitivity near EPs. The requirements for $\beta(t)$ are summarized below,

$$\lim_{t \rightarrow \tau_p} 1 - \beta^2(t) = 0^+ \quad \text{and} \quad \lim_{t \rightarrow \tau_p} \dot{\beta}(t) = 0. \quad (5)$$

Notably, in contrast to previous schemes, the amplification effects are now decoupled from the magnitude of the measured parameter (e.g., $\dot{\Phi}$) while remaining independently tunable via the ratio of γ to $J(t)$.

Chirality and non-reciprocity.— The tunneling behavior can be characterized by the stability of the differential equations Eq.(3), as the local dynamics near a given time instant

can be approximated as a linear time-invariant (LTI) system due to slow parameter variation [36]. The real part of the eigenvalues λ_{\pm} of the matrix $\mathbf{M} = i(\mathbf{A}^{\mathcal{CPT}} - \mathbf{H}^{\mathcal{CPT}})$ is $\text{Re } \lambda_{\pm} \approx \pm \gamma (J(t)^2 - \gamma^2) \dot{\Phi}(t)/(4 (J(t)^2 - \gamma^2)^3 - \gamma^2 J(t)^2)^{1/2}$. Under the condition in Eq.(5), $\text{Re } \lambda_{\pm} \gg 0$ indicates rapid divergence of the system state. The nontrivial term, manifesting as a factor characterized by chirality and non-reciprocal topology, emerges as the diagonal elements of $\mathbf{A}^{\mathcal{CPT}}$. The diagonal terms can be written as

$$\mathcal{A}_{nn}^{\mathcal{CPT}}(t) = \frac{(-1)^n i \gamma}{2\sqrt{J(t)^2 - \gamma^2}} \text{sgn}(\dot{\Phi}(t)) \cdot |\dot{\Phi}(t)| - \frac{\dot{\Phi}(t)}{2}, \quad (6)$$

where $\mathcal{A}_{11}^{\mathcal{CPT}}(t) = -\mathcal{A}_{22}^{\mathcal{CPT}}(t)$ is determined by the intraband Berry connection with $\mathcal{A}_{nn}^{\mathcal{CPT}}(t) = \dot{\kappa}(t) \mathcal{A}_j^{mn} \mathcal{CPT}$ [34]. In these two terms, the imaginary part induced by dissipation rate γ leads to phase-neutral geometric gain ($\text{Im} \mathcal{A}_{nn}^{\mathcal{CPT}} > 0$) or loss effect ($\text{Im} \mathcal{A}_{nn}^{\mathcal{CPT}} < 0$) [37, 38], which depends on both the direction of change of the parameter $\Phi(t)$ and initial n th eigenstate (e.g., $\text{sgn}(\dot{\Phi}(t))$ and $(-1)^n$). This effect leads to *chiral* and *nonreciprocal* tunneling, as the tunneling always occurs in the geometric loss regime, as shown in Fig. 1(c).

(i) Chirality is defined as follows. Starting from the same

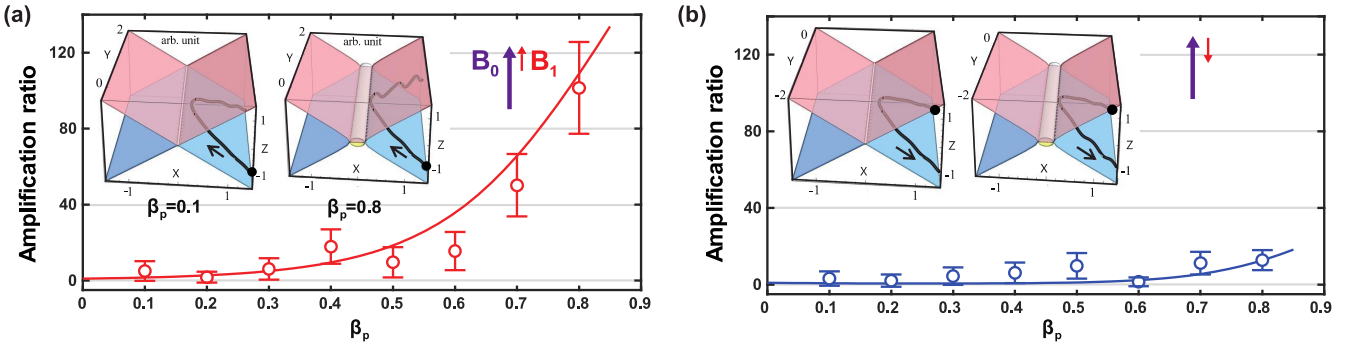


FIG. 3. Experimental results for critically enhanced topological tunneling. (a) In the main figure, the solid curves represent theoretical predictions and the points with error bars represent experimental data. The X-axis represents the coupling strength J in the Hamiltonian $H_{\mathcal{PT}}(t)$, the Y-axis represents the phase Φ , and the Z-axis represents the eigenvalue magnitude. The red surface shows the eigenvalue surface of the eigenstate $|\phi_1\rangle$, the blue surface shows the eigenvalue surface of $|\phi_2\rangle$. The yellow and gray surfaces show the imaginary parts of eigenvalues for $|\phi_2\rangle$ and $|\phi_1\rangle$ respectively when \mathcal{PT} symmetry is broken. The black circles represent the initial state. The black arrows indicate the evolution direction of quantum states. The state is initialized in $|\phi_2\rangle$ with $d\Phi(t)/dt > 0$. (b) The state is initialized in $|\phi_2\rangle$ with $d\Phi(t)/dt < 0$.

eigenstate with the fixed value of n , clockwise (CW: Φ increasing over time, $\text{sgn}(\dot{\Phi}(t)) > 0$) and counterclockwise (CCW: Φ decreasing over time, $\text{sgn}(\dot{\Phi}(t)) < 0$) evolutions exhibit different tunneling effects. This asymmetry arises because $\text{Im}(\text{CW}(\mathcal{A}_{nn}^{\mathcal{CPT}})) = -\text{Im}(\text{CCW}(\mathcal{A}_{nn}^{\mathcal{CPT}}))$, where $\text{Im}()$ denote the imaginary part.

(ii) We can also define non-reciprocity. When considering the combined action of CW and CCW processes, the aforementioned relationship leads to a non-reciprocal behavior $\text{Im}(\text{CCW}(\text{CW}(\mathcal{A}_{nn}^{\mathcal{CPT}}))) = -\text{Im}(\text{CW}(\text{CCW}(\mathcal{A}_{nn}^{\mathcal{CPT}})))$. This means the state exchange is forbidden in the time-reversed process [39].

Experimental execution— The sensitivity of this tunneling depends not only on $\dot{\Phi}(t)$ with its criticality-enhanced amplification factor $\xi(t)$, but also on the chiral and non-reciprocal response to the sign of $\dot{\Phi}(t)$. This unique combination of the above features could potentially enable non-Hermitian vector sensing. Here, we consider the simplest case with constant detuning, i.e., $\dot{\Phi}(t) = \Delta$. Thus the sign of Δ determines the direction of $\dot{\Phi}(t)$. For a magnetically sensitive energy level, Δ represents the frequency shift between the energy level and the driving field caused by the magnetic field fluctuations $|\Delta| = |\eta(\vec{B}_0 + \delta\vec{B}) + \omega_0 - \omega_{\text{field}}|$ in direction of \vec{B}_0 , where η is the Zeeman coefficient, \vec{B}_0 is the applied static magnetic field, $\delta\vec{B}$ is the magnetic field to be measured at the projection of \vec{B}_0 , ω_0 is two-level resonance frequency, and ω_{field} is driven frequency. Considering the resonance condition $\eta\vec{B}_0 + \omega_0 - \omega_{\text{field}} = 0$, the sign and value of Δ can be attributed to a small magnetic field $\vec{B}_1 = \delta\vec{B}$, whose magnitude and direction both have significant effects on the system. Based on this, the following vector relationship can be defined $\vec{\Delta} = \eta\vec{B}_1$. Therefore \vec{B}_1 can be estimated by measuring $\vec{\Delta}$.

To achieve the criticality-enhanced effect of $\vec{\Delta}$, we satisfy the condition in Eq. (5) through the modulation function $J(t) = (J_l - J_p) \cos(\pi t/T + \pi/2) + J_l$. For a clearer mani-

festation of critical behavior, we normalize $J(t)$ by γ

$$\frac{1}{\beta(t)} = \left(\frac{1}{\beta_l} - \frac{1}{\beta_p} \right) \cos(\pi t/T + \pi/2) + \frac{1}{\beta_l}. \quad (7)$$

The parameters $\beta_p = \gamma/J_p$ and $\beta_l = \gamma/J_l$ represent the ‘pin’ of the ‘probe’ close to the EP line ($\beta = 1$) and the ‘tail’ of the ‘probe’ away from the EP line, respectively. By adjusting γ , we can control the position of the ‘pin’ relative to the EP line within the \mathcal{PT} -symmetric regime, as shown in Fig. 2(a). Here, we set the parameters to $J_p = 4 \times 2\pi$ kHz, $J_l = 30 \times 2\pi$ kHz, and total time $T = 2\tau_p = 200 \mu\text{s}$.

Experimentally, we implemented this scheme using a single trapped $^{171}\text{Yb}^+$ ion. The relevant energy level structure is shown in SM [34]. To demonstrate the non-Hermitian amplified sensitivity, we first prepare the initial state as $|\phi_2(0)\rangle$ (i.e., $|-x\rangle$) with $\Phi(0) = 0$ by applying a $\pi/2$ pulse to $|0\rangle$; then separately apply the modulated $H_{\mathcal{PT}}(t)$ under the Hermitian conditions $\beta_p = 0$ (by setting $\gamma = 0$) and non-Hermitian conditions $\beta_p = 0.75$ (by setting $\gamma = 0.75J_p$), while varying the norm of $\vec{\Delta}$ (denoted as Δ) via an arbitrary waveform generator; finally, we observe the response of the system by measuring the populations of $|1\rangle$, denoted as P_z . The corresponding experimental results are presented in Fig. 2(b) and Fig. 2(c). In the Hermitian case, since the modulation rate of $J(t)$ of $H_{\mathcal{PT}}(t)$ satisfies the adiabatic condition $\left| \frac{j(t)\Delta}{(\Delta^2 + j(t)^2)^{3/2}} \right| \ll 1$, the evolution remains adiabatic [34]. Consequently, the final state preserves its initial form $|-x\rangle$ (evidenced by the outcome $P_z \approx 0.5$), which is guaranteed by the periodic boundary condition $J(T) = J(0) \gg \Delta$. This adiabatic characteristic fundamentally prohibits the detection of Δ in the current modulation function. In the non-Hermitian case, tunneling can occur even for small Δ . As Δ increases, the onset of tunneling shifts closer to the ‘pin’, which demonstrates the heightened sensitivity to variations in Δ . Conversely, the Δ can be measured by observing the degree of tunneling completion, i.e., P_z . If

The tunneling is not completed, P_z will oscillate for different values of Δ at the final time T , as shown in Fig. 2(c). Figure 2(d) presents the value of P_z at time T , revealing a pronounced distinction between Hermitian and non-Hermitian regimes.

We further explore the geometric amplification by varying β_p in Eq. (7), examining not only the initial states $|\phi_1(0)\rangle$ and $|\phi_2(0)\rangle$, but also the sign of Δ . To quantify the sensitivity, we use Classical Fisher Information (CFI), which is defined as $I(\theta) = (1/N_\theta) \sum_{j=1}^{N_\theta} \left[(dP_z/d\theta_j)^2 / P_z \right]$. Here θ_j represents the parameterized signal to which the system responds, with $\Phi(t)$ as the parameter, and N_θ is the number of sampling points for θ_j . To further characterize the geometric amplification, we employ the amplification ratio, I_{β_p}/I_0 , where I_{β_p} and I_0 denote the CFI for a given value of β_p and for $\beta_p = 0$, respectively. As shown in Fig. 3, the amplification ratio exhibits a divergence due to the critical effect, and this enhancement is selectively dependent on the initial state and the sign of Δ . Results for the initial state $|\phi_1\rangle$ are presented in SM [34]. We note that as β_p increases, the slight increase in amplification ratio in Fig. 3(b) originates from minor non-adiabatic oscillations caused by rapid parameter modulation, whereas no tunneling occurs during this process. The experimental results discussed above are in excellent agreement with the trend of the critical and chiral response function described by Eq. (4) and Eq. (6). This consistency highlights the potential of the system as a vector quantum sensing with high sensitivity.

This study demonstrates the first investigation of non-adiabatic non-Hermitian quantum sensing through transient dynamics near EPs. The key insight lies in the tunneling behavior of non-Hermitian systems, which is driven by the divergence of the quantum metric near EPs. Furthermore, this tunneling induces chiral and non-reciprocal response characteristics, enabling high-resolution detection and discrimination of vector signals along a one-dimensional direction. The CFI results validate these features. Our research not only advances the theoretical framework of non-Hermitian sensing but also paves the way for experimental studies of non-Hermitian critical effects mediated by the quantum metric. Exploring this scheme in higher-order EP regimes is a promising future direction.

The authors thank Prof Mang Feng, Dr. Konghao Sun for helpful discussions, and acknowledge Dr. Xinxin Rao and Mingshen Li for experimental support. This work is supported by the National Key Research and Development Program of China, “Gravitational Wave Detection” Special Project under Grant No. 2022YFC2204402, the National Natural Science Foundation of China under Grants No. 12074439 and No. 12304315, Guangdong Provincial Quantum Science Strategic Initiative under Grants No. GDZX2203001 and No. GDZX2303003, and Shenzhen Science and Technology Program under Grant No. JCYJ20220818102003006.

- [1] Kun Ding, Chen Fang, and Guancong Ma. Non-hermitian topology and exceptional-point geometries. *Nature Reviews Physics*, 4(12):745–760, 2022.
- [2] Aqiang Guo, Greg J Salamo, David Duchesne, Roberto Morandotti, Maite Volatier-Ravat, Vincent Aimez, Georgios A Siviloglou, and Demetrios N Christodoulides. Observation of pt-symmetry breaking in complex optical potentials. *Physical review letters*, 103(9):093902, 2009.
- [3] WD Heiss. Exceptional points of non-hermitian operators. *Journal of Physics A: Mathematical and General*, 37(6):2455, 2004.
- [4] Hossein Hodaei, Absar U Hassan, Steffen Wittek, Hipolito Garcia-Gracia, Ramy El-Ganainy, Demetrios N Christodoulides, and Mercedeh Khajavikhan. Enhanced sensitivity at higher-order exceptional points. *Nature*, 548(7666):187–191, 2017.
- [5] Tosio Kato. *Perturbation theory for linear operators*, volume 132. Springer Science & Business Media, 2013.
- [6] Yulin Wu, Peiji Zhou, Ting Li, Weishi Wan, and Yi Zou. High-order exceptional point based optical sensor. *Optics Express*, 29(4):6080–6091, 2021.
- [7] Romain Fleury, Dimitrios Sounas, and Andrea Alu. An invisible acoustic sensor based on parity-time symmetry. *Nature communications*, 6(1):5905, 2015.
- [8] Weijian Chen, Şahin Kaya Özdemir, Guangming Zhao, Jan Wiersig, and Lan Yang. Exceptional points enhance sensing in an optical microcavity. *Nature*, 548(7666):192–196, 2017.
- [9] Jing Zhang, Bo Peng, Şahin Kaya Özdemir, Kevin Pichler, Dmitry O Krimer, Guangming Zhao, Franco Nori, Yu-xi Liu, Stefan Rotter, and Lan Yang. A phonon laser operating at an exceptional point. *Nature Photonics*, 12(8):479–484, 2018.
- [10] Zhicheng Xiao, Huanan Li, Tsampikos Kottos, and Andrea Alù. Enhanced sensing and nondegraded thermal noise performance based on pt-symmetric electronic circuits with a sixth-order exceptional point. *Physical Review Letters*, 123(21):213901, 2019.
- [11] Xizhou Shen, Keyu Pan, Xiumei Wang, Hengxuan Jiang, and Xingping Zhou. Gain and loss induced higher-order exceptional points in a non-hermitian electrical circuit. *Journal of Physics D: Applied Physics*, 57(6):065102, 2023.
- [12] Shuo Liu, Shaojie Ma, Cheng Yang, Lei Zhang, Wenlong Gao, Yuan Jiang Xiang, Tie Jun Cui, and Shuang Zhang. Gain-and loss-induced topological insulating phase in a non-hermitian electrical circuit. *Physical Review Applied*, 13(1):014047, 2020.
- [13] Liangyu Ding, Kaiye Shi, Qiuxin Zhang, Danna Shen, Xiang Zhang, and Wei Zhang. Experimental determination of pt-symmetric exceptional points in a single trapped ion. *Physical Review Letters*, 126(8):083604, 2021.
- [14] Yang Wu, Wenquan Liu, Jianpei Geng, Xingrui Song, Xiangyu Ye, Chang-Kui Duan, Xing Rong, and Jiangfeng Du. Observation of parity-time symmetry breaking in a single-spin system. *Science*, 364(6443):878–880, 2019.
- [15] Shang Yu, Yu Meng, Jian-Shun Tang, Xiao-Ye Xu, Yi-Tao Wang, Peng Yin, Zhi-Jin Ke, Wei Liu, Zhi-Peng Li, Yuan-Ze Yang, et al. Experimental investigation of quantum pt-enhanced sensor. *Physical Review Letters*, 125(24):240506, 2020.
- [16] Hoi-Kwan Lau and Aashish A Clerk. Fundamental limits and non-reciprocal approaches in non-hermitian quantum sensing. *Nature communications*, 9(1):4320, 2018.
- [17] Alexander McDonald and Aashish A Clerk. Exponentially-

enhanced quantum sensing with non-hermitian lattice dynamics. *Nature communications*, 11(1):5382, 2020.

[18] Lei Xiao, Yaoming Chu, Quan Lin, Haiqing Lin, Wei Yi, Jianming Cai, and Peng Xue. Non-hermitian sensing in the absence of exceptional points. *Physical Review Letters*, 133(18):180801, 2024.

[19] Pengfei Lu, Yang Liu, Qifeng Lao, Teng Liu, Xinxin Rao, Ji Bian, Hao Wu, Feng Zhu, and Le Luo. Dynamical topology of chiral and nonreciprocal state transfers in a non-hermitian quantum system. *Communications Physics*, 8(1):91, 2025.

[20] Thomas J Milburn, Jörg Doppler, Catherine A Holmes, Stefano Portolan, Stefan Rotter, and Peter Rabl. General description of quasiadiabatic dynamical phenomena near exceptional points. *Physical Review A*, 92(5):052124, 2015.

[21] Jörg Doppler, Alexei A Mailybaev, Julian Böhm, Ulrich Kuhl, Adrian Girschik, Florian Libisch, Thomas J Milburn, Peter Rabl, Nimrod Moiseyev, and Stefan Rotter. Dynamically encircling an exceptional point for asymmetric mode switching. *Nature*, 537(7618):76–79, 2016.

[22] Wenquan Liu, Yang Wu, Chang-Kui Duan, Xing Rong, and Jiangfeng Du. Dynamically encircling an exceptional point in a real quantum system. *Physical Review Letters*, 126(17):170506, 2021.

[23] Xu-Lin Zhang and Che Ting Chan. Dynamically encircling exceptional points in a three-mode waveguide system. *Communications Physics*, 2(1):63, 2019.

[24] Hadiseh Nasari, Gisela Lopez-Galmiche, Helena E Lopez-Aviles, Alexander Schumer, Absar U Hassan, Qi Zhong, Stefan Rotter, Patrick LiKamWa, Demetrios N Christodoulides, and Mercedeh Khajavikhan. Observation of chiral state transfer without encircling an exceptional point. *Nature*, 605(7909):256–261, 2022.

[25] Hailong Wang, Li-Jun Lang, and Yi Dong Chong. Non-hermitian dynamics of slowly varying hamiltonians. *Physical Review A*, 98(1):012119, 2018.

[26] S Ibáñez and JG Muga. Adiabaticity condition for non-hermitian hamiltonians. *Physical Review A*, 89(3):033403, 2014.

[27] LALE Landau, Evgeny Lifshitz, et al. On the theory of the dispersion of magnetic permeability in ferromagnetic bodies. *Phys. Z. Sowjetunion*, 8(153):101–114, 1935.

[28] NV Vitanov. Transition times in the landau-zener model. *Physical Review A*, 59(2):988, 1999.

[29] Sota Kitamura, Naoto Nagaosa, and Takahiro Morimoto. Non-reciprocal landau–zener tunneling. *Communications Physics*, 3(1):63, 2020.

[30] Jing Yang, Shengshi Pang, and Andrew N Jordan. Quantum parameter estimation with the landau-zener transition. *Physical Review A*, 96(2):020301, 2017.

[31] Carl M Bender. Making sense of non-hermitian hamiltonians. *Reports on Progress in Physics*, 70(6):947, 2007.

[32] Carl M Bender, Dorje C Brody, Hugh F Jones, and Bernhard K Meister. Faster than hermitian quantum mechanics. *Physical Review Letters*, 98(4):040403, 2007.

[33] Pengfei Lu, Teng Liu, Yang Liu, Xinxin Rao, Qifeng Lao, Hao Wu, Feng Zhu, and Le Luo. Realizing quantum speed limit in open system with a pt-symmetric trapped-ion qubit. *New Journal of Physics*, 26(1):013043, 2024.

[34] Supplemental material.

[35] O Bleu, G Malpuech, Y Gao, and DD Solnyshkov. Effective theory of nonadiabatic quantum evolution based on the quantum geometric tensor. *Physical Review Letters*, 121(2):020401, 2018.

[36] Hassan K Khalil and Jessy W Grizzle. *Nonlinear systems*, volume 3. Prentice hall Upper Saddle River, NJ, 2002.

[37] Michael Victor Berry. Quantal phase factors accompanying adiabatic changes. *Proceedings of the Royal Society of London. A. Mathematical and Physical Sciences*, 392(1802):45–57, 1984.

[38] Shi-Dong Liang and Guang-Yao Huang. Topological invariance and global berry phase in non-hermitian systems. *Physical Review A—Atomic, Molecular, and Optical Physics*, 87(1):012118, 2013.

[39] Christophe Caloz, Andrea Alu, Sergei Tretyakov, Dimitrios Sounas, Karim Achouri, and Zoé-Lise Deck-Léger. Electromagnetic nonreciprocity. *Physical Review Applied*, 10(4):047001, 2018.